

Theoretical modeling of single quantum dot photodiodes

Matthias Sabathil¹, S. Hackenbuchner, S. Birner, D. Mamaluy, J. A. Majewski, P. Vogl

Semiconductor quantum dots (QDs) are often referred to as artificial atoms due to their discrete energy levels. Because of the possibility to influence the size and composition of these quantum dots, their energy levels are not fixed like in real atoms, but may be tuned into some desired energy range. To obtain information about the optical properties of a QD one can perform various kinds of experiments, e.g. photoluminescence or photocurrent measurements. In order to understand the physics involved, these measurements need to be supplemented by a theoretical analysis. We have employed our recently developed simulation tool *nextnano*³ and used it to perform detailed theoretical studies of an $\text{In}_{0.5}\text{Ga}_{0.5}\text{As}$ QD-structure that has been grown in the WSI. The simulator is an ideal tool to calculate the electronic structure as well as the realistic spatial strain distribution. The resulting wave functions provide information about the exciton energies, the optical matrix elements and the tunneling rates for electrons and holes.

The device we focus on consists of a GaAs n-i structure with $\text{In}_{0.5}\text{Ga}_{0.5}\text{As}$ QDs embedded within the intrinsic region. Excitons are optically generated inside the quantum dot and can escape via a tunneling process for sufficiently high electric fields. The dependence of the photocurrent and the exciton energy on the electric field (Stark-effect)

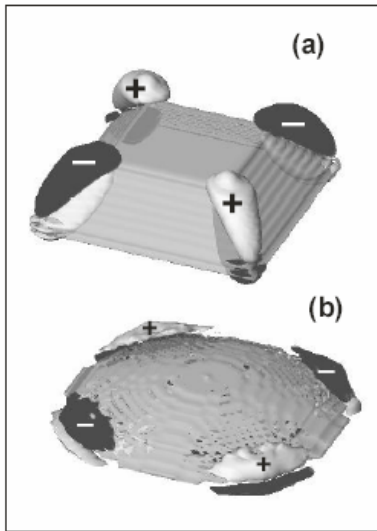


Fig. 1: Localization of the piezo charges for different quantum dot shapes. (Truncated pyramids (a) and lens shaped dots (b)).

has been measured experimentally. Since the quantum dots are buried inside the structure, however, their shape and alloy composition is unknown. With our model calculations, we have assumed various kinds of geometrical shapes and alloy profiles and then compared the resulting predicted optical properties with the experimentally measured ones. It turns out that the geometry of the QD has a drastic impact on the magnitude and localization of the piezoelectric charges that occur due to deformation of the lattice in the QD. In Fig. 1 we show the distribution of the piezoelectric charges for (a) a pyramidal shaped and (b) a lens shaped QD, respectively. In the pyramidal dot, the piezo charges form dipoles that are located mainly along the edges and reach into the interior of the QD, whereas in the lens shaped dot the charges are more evenly spread out and lie further away from the center of the dot. The piezoelectric charges add to the confining potential and therefore affect the wave functions of the electrons and holes. Fig. 2 shows the electron (light) and hole (dark) ground state wave function for the two different QD geometries. Due to

the small effective mass, the electron wave function is only weakly influenced by the piezoelectric charges and remains in the center of the dot for both geometries. By contrast, the shape of the hole wave function is strongly governed by the piezoelectric potential and

¹ Phone: +49-89-289-12762, email: sabathil@wsi.tum.de

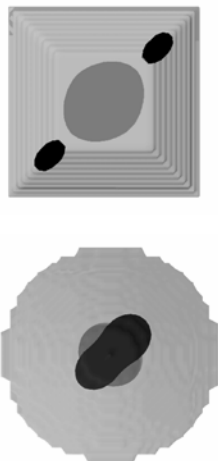


Fig. 2:
Localization of electron (light) and hole (dark) wave functions.

the center of its wave function is located mainly in the minimum of the potential whereas the electron wave function, which has a much higher kinetic energy, remains delocalized. The separation of the center of the hole wave function from the center of the electron wave function results in a ‘built in’ charge dipole along the growth axis. This ‘built in’ dipole moment manifests itself in the experimentally measured change of the exciton energy as a function of the electric field (Stark-shift), which can be explained by the interaction of the electric field with the dipole moment of the exciton. The two parts that contribute to this dipole moment are the field induced dipole which results in a quadratic Stark-shift and the ‘built in’ dipole that accounts for a linear dependence on the field. In Fig. 3 we compare the experimentally measured stark shift of the real QD with calculations assuming a constant alloy profile (a) and a Gaussian profile with a maximum Indium concentration at the tip of the QD. The experimental curve exhibits a large ‘built in’ dipole that, according to our calculations, can only be matched by assuming a highly nonlinear alloy profile such as the one assumed in Fig. 3 (b).

We showed that our calculations yield detailed information about the shape and alloy composition of a QD which cannot easily be measured directly. Furthermore, we are able to predict additional experimentally accessible quantities such as optical matrix elements or tunneling rates for electrons and holes in QDs.

exhibits fundamental differences between the two QDs. In the lens shaped dot, the hole wave function is slightly distorted in direction of the diagonal but remains in the center of the dot. In the pyramidal dot, on the other hand, the hole ground state is mainly localized in two corners because of the attracting piezoelectric charges along the corresponding edges.

An important quantity, which determines the efficiency of the optical exciton generation, is the spatial overlap of the electron and hole wave function. Since a high efficiency is a prerequisite to measure any photocurrent we can assume that the real QD is lens shaped rather than pyramidal shaped.

In addition to the shape, we need to determine the alloy composition of the QD which may be spatially inhomogeneous since the dot does not consist of pure Indium. Again, with the aid of the simulator, we can test various alloy composition profiles. Since the confining potential is mainly a function of the alloy composition, the localization of the electron and hole wave functions along the growth axis will be influenced by the alloy composition profile in an analogous way as their lateral position was determined by the piezoelectric charges. Due to the heavy effective mass of the hole,

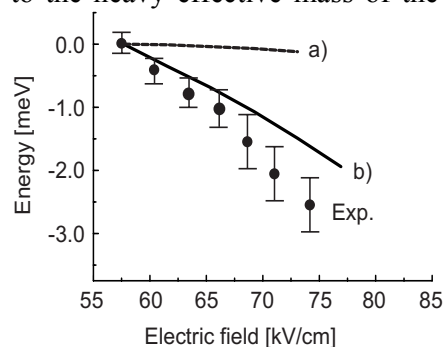


Fig. 3: *Experimental Stark-shift compared to calculations assuming constant (a) and nonlinear (b) alloy profile.*